



Model scale tunnel fire tests on maximum ceiling gas temperature for structural protection

Ying Zhen Li, Haukur Ingason

RISE Rapport 2018:58

Model scale tunnel fire tests on maximum ceiling gas temperature for structural protection

Ying Zhen Li, Haukur Ingason

Abstract

Model scale tunnel fire tests on maximum ceiling gas temperature for structural protection

Model scale tests with varying materials as tunnel structure were carried out to further study the theoretical model of maximum gas temperature for structural protection. New correlation for calculation of air mass flow rate is introduced. Test results showed that the maximum ceiling gas temperatures increases with the increasing heat release rate and decreases with the increasing tunnel width and thermal inertia of the tunnel linings. Higher ventilation velocity may also result in slightly higher temperatures for large fires.

Comparisons of model scale tests and theoretical models showed that the theoretical models predict the maximum ceiling gas temperature very well. A fire with a fixed heat release rate or a time-varying heat release rate, the effects of tunnel structure, tunnel ventilation, tunnel width and fire size have been well considered by the model. Comparisons of other model and full scale tests with theoretical models further verified this.

Key words: tunnel, fire, temperature, scale model, linings, ventilation

RISE Research Institutes of Sweden

RISE Rapport 2018:58
ISBN 978-91-88907-02-8
ISSN 0284-5172
Borås 2018

Table of contents

Abstract	3
Table of contents	4
Preface	5
Summary	6
1 Introduction	7
2 Theoretical model	9
2.1 New MT model	9
2.2 Theoretical considerations.....	10
2.2.1 Heat transfer coefficient	10
2.2.2 Parameter K_{ef}	12
2.2.3 Mass flow rate	12
2.2.4 Time correction	14
3 Model scale tunnel fire tests	16v
3.1 Tunnel	16
3.2 Fire source.....	17
3.3 Ventilation.....	17
3.4 Measurement	17
3.5 Test procedure	19
4 Results and discussions	20
4.1 Test results	20
4.1.1 Influence of tunnel structure materials	20
4.1.2 Influence of fire size.....	21
4.1.3 Influence of ventilation	22
4.1.4 Influence of tunnel width	23
4.2 Comparisons to theoretical models	24
4.2.1 Calculation of heat transfer coefficient	24
4.2.2 Tunnel structure and ventilation.....	25
4.2.3 Tunnel width	27
4.2.4 Fire size HRR.....	28
4.2.5 Pool fires with varying HRRs	29
4.3 Comparison to other model scale tests.....	30
4.4 Comparison to full scale tests.....	31
4.5 Summary of the new MT model	33
5 Conclusions	34
Reference	35

Preface

The research work presented in this report was sponsored by TUSC Tunnel Underground Safety Center. The financiers of TUSC are the Swedish Transport Administration, the Swedish Fortifications Agency, the Swedish Nuclear Fuel and Waste Management Company (SKB) and RISE Research Institutes of Sweden.

The technicians Emil Norberg, Michael Magnusson, Tarmo Karjalainen, Sven-Gunnar Gustafsson, Jonathan Backlund are greatly acknowledged for the assistance in conducting the tests.

Summary

Numerous tests with varying materials as tunnel structure were carried out to further study the theoretical model of maximum gas temperature for structural protection recently presented by the authors [1]. New correlation for calculation of air mass flow rate is introduced.

Analysis of the test results showed that the maximum gas temperatures are higher for a more fire-resistant material (with a lower thermal inertia) with the same heat release rate. The maximum gas temperature increases with the increasing heat release rate, but this increase becomes smaller as the heat release rate continues to rise. This increase depends on the ventilation velocity, and it is smaller for a lower velocity. The influence of different ventilation conditions tested is not significant. It appears that higher ventilation velocity may result in slightly higher temperatures for large fires. The maximum gas temperature decreases with the increasing tunnel width due to greater heat loss to environment. Overall, the maximum ceiling gas temperatures increases with the increasing heat release rate and decreases with the increasing tunnel width and thermal inertia of the tunnel linings.

Comparisons of model scale tests and theoretical models showed that the theoretical models predict the maximum ceiling gas temperature very well, whether it is a fire with a fixed heat release rate or a time-varying heat release rate. The effects of tunnel structure, tunnel ventilation velocity, tunnel width and fire size have been well considered by the model. Comparisons of other model and full scale tests with theoretical models further verified this.

1 Introduction

Gas temperature is an important parameter to consider when designing the fire resistance of a tunnel structure. It can be expected that tunnel linings (e.g. rock, concrete) may have influence on the maximum temperature.

In the past decade, Li et al. [2] and Li and Ingason [3] developed a method for calculating excess ceiling gas temperature as a function of these parameters, which can produce time-temperature curves using realistic HRRs (design fires). Alternatively, through comparison with the obtained time-temperature curve, a standardised time-temperature curve, e.g. the HC curve, can be selected for use in a specific project. The temperature value obtained can be used to calculate the heat flux that the structure is exposed to, and the temperature inside the structure can be calculated as a function of the distance from its exterior surface. The internal temperature of the reinforced bars of a concrete tunnel structure can be calculated; when it reaches a certain, critical value, the time to failure can be determined. In their models [2, 3], a value of 1350 °C is used for maximum ceiling excess gas temperature based on large scale test data. However, through analysis of test data, it has been observed that gas temperature does not increase as rapidly above 800 - 1000 °C, that is, it takes significantly long time for gas temperatures to reach maximum values above this level [1]. Figure 1 shows a comparison of the test data and the predictions according to Li et al's model [2, 3]. Clearly, for gas temperature over approx. 800 °C, there appears to be a time delay for the gas temperature to reach a higher temperature.

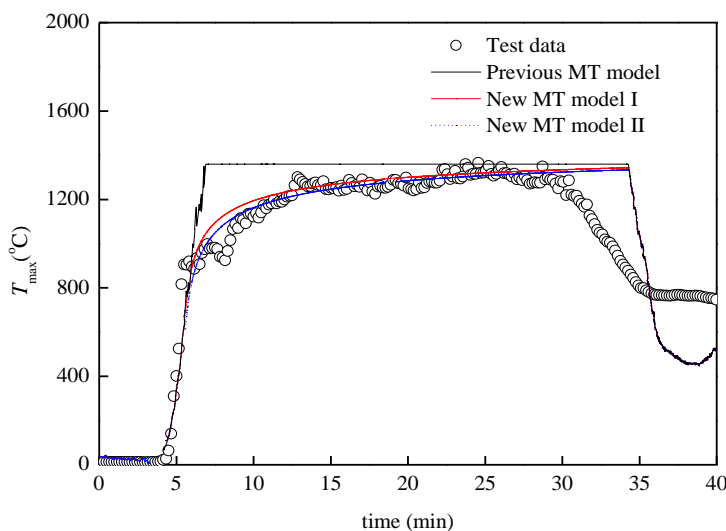


Figure 1 A comparison of the previous and new models for Runehamar test 1.

Thereafter, Li and Ingason [1] redeveloped their model for maximum ceiling gas temperatures taking the influence of tunnel linings into account. The models have been validated to a large extent using existing test data (e.g. the comparisons shown in Figure 1), but some parameters still need to be tuned in and further validated. More detailed introduction can be found in Li and Ingason [1].

In present work, a series of model scale tests was carried out to investigate the ceiling gas temperatures in tunnels of various lining types. The parameters tested also include tunnel cross sections, ventilation conditions and fire sources. This was thought to be necessary before drawing

too extended conclusions about the role of type of lining on the final gas temperatures inside tunnels.

2 Theoretical model

The new model for maximum ceiling gas temperatures developed by Li and Ingason [1] is shortly depicted here as the basis of this study.

2.1 New MT model

The maximum excess gas temperature beneath the tunnel ceiling is expressed as follows:

$$\Delta T_{\max} = \min(\Delta T_{\text{previous}}, \Delta T) \quad (1)$$

where $\Delta T_{\text{previous}}$ is the maximum excess gas temperature based on the previous model [2, 3]:

$$\Delta T_{\text{previous}} = \min\left(17.5 \frac{\dot{Q}^{2/3}}{H_{ef}^{5/3}}, \frac{\dot{Q}}{u_o b_{fo}^{1/3} H_{ef}^{5/3}}\right) \quad (2)$$

where \dot{Q} is heat release rate, H_{ef} is effective tunnel height, u_o is velocity, and b_{fo} is equivalent fire radius.

The maximum excess gas temperature according to the new model, ΔT , based on a simple energy balance consideration, is expressed as follows:

$$\Delta T(t) = \frac{\Delta T_{ad} - \varphi \varepsilon \sigma A (T(t)^4 - T_o^4) / [\dot{m}_g(t) c_p]}{1 + h(t_c) / K_{ef}} \quad (3)$$

where \dot{m}_g is mass flow rate of the flame volume, A is tunnel cross-sectional area, c_p is heat capacity, h is heat transfer coefficient, K_{ef} is a parameter defined in Eq. (15), and φ is a correction factor (1 by default), ε is the emissivity of the flame volume. In full scale large tunnel fires, the emissivity is around 1 [4]. In the model scale, an effective emissivity obtained via testing can be used. ΔT_{ad} is the adiabatic flame temperature of 1580 °C [1].

The analytical solution for the correlation, in a form of $a_1 T^4 + T - a_2 = 0$, can be expressed as follows:

$$T = \frac{1}{2} \sqrt{\frac{3.494 a_2}{a_1^{1/3} (9 + \omega)^{1/3}} - \frac{(9 + \omega)^{1/3}}{2.622 a_1^{2/3}} + \frac{4.079}{a_1 \psi}} - \frac{\psi}{4.079} \quad (4)$$

where

$$\omega = \sqrt{3} \sqrt{27 + 256 a_1 a_2^3}, \quad \psi = \sqrt{\frac{(18 + 2\omega)^{2/3} - 14.537 a_1^{1/3} a_2}{a_1^{2/3} (9 + \omega)^{1/3}}}$$

$$a_1 = \frac{\sigma A / \dot{m}_g c_p}{1 + h_k / K_{ef}}, \quad \text{and} \quad a_2 = \frac{\Delta T_{ad} + \sigma A T_o^4 / \dot{m}_g c_p}{1 + h_k / K_{ef}} + T_o$$

Alternatively, an explicit time-marching procedure can be used; i.e. the temperature at the previous stage (t) can be used to estimate the temperature at this stage ($t + dt$):

$$\Delta T(t + dt) = \frac{\Delta T_{ad} - \varphi \varepsilon \sigma A [T(t)^4 - T_o^4] / \dot{m}_g c_p}{1 + h_k(t_c) / K_{ef}} \quad (5)$$

In this process, the gas temperature at the previous stage, $T(t)$, is used to estimate the radiation loss in order to obtain the excess temperature at the new stage, $\Delta T(t + dt)$. Ordinarily, an interval of 10 seconds can be used without producing any large error. This time-marching procedure can be performed easily using an excel sheet.

For manual calculation, a gas temperature can be assumed for T on the right-hand side, and then a new gas temperature T can be obtained. After repeating this simple procedure twice, an approximate solution can be obtained.

2.2 Theoretical considerations

2.2.1 Heat transfer coefficient

Simplified expression

In calculation of the heat transfer coefficient, it is commonly assumed that the conduction heat transfer dominates the process for large fires in tunnels. Therefore, the heat transfer coefficient is estimated as follows by default:

$$h \approx h_k = \sqrt{\frac{k \rho c}{\pi t}} \quad (6)$$

Note that the thermal inertia of the material, I , is defined as $I = \sqrt{k \rho c}$. So this heat transfer coefficient is directly proportional to the thermal inertia of the material. The reasonability of directly using Eq. (6) as the heat transfer coefficient will be examined in Section 4.2.1.

Full expression

At the early stage, the convection heat transfer and radiation heat transfer may have some influence. An analysis of the combined heat transfer is presented below.

A tunnel wall can be considered as an infinite plate consisting of concrete linings, given that the heat penetration to the backside of the lining generally takes a long time. The electrical circuit analog of the overall heat transfer from the gas to the wall surface is shown in Figure 2.

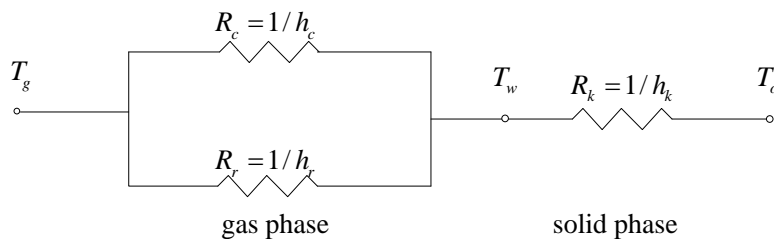


Figure 2 The electrical circuit analog of global heat transfer from gas to the wall.

Note that the thermal resistances are the reciprocals of the heat transfer coefficients. Therefore, the overall heat flux through the surface can be expressed as:

$$\dot{q}'' = \frac{T_g - T_o}{1/h_k + 1/(h_c + h_r)} \quad (7)$$

In other words, the heat transfer coefficient, h , can be estimated by the following equation:

$$h = \frac{1}{1/h_k + 1/(h_c + h_r)} \quad (8)$$

The convective heat transfer coefficient, h_c , could be expressed as follows:

$$h_c = \frac{k}{l} 0.037 \text{Re}^{4/5} \text{Pr}^{0.43} \quad (9)$$

where the Reynolds number and the Prandtl number, Pr , are defined as:

$$\text{Re} = \frac{ul}{\nu}, \quad \text{Pr} = \frac{\nu}{a}$$

The radiative heat flux on the wall surface may be expressed as:

$$h_r = \sigma(T_g^2 + T_w^2)(T_g + T_w) / (1/\varepsilon_g + 1/\varepsilon_w - 1) \quad (10)$$

where the subscripts c , k and r indicate convective, conductive and radiative heat transfer respectively. Note that the conductive heat transfer coefficient, h_k , increases very rapidly with time. Further, the radiative heat transfer coefficient, h_r , may vary significantly with time.

Thermally thin materials

In some tests performed here, steel was applied which needs special treatment as it is thermally thin material and its back side also transfers heat by convection and radiation. In the following, an analysis of heat transfer process for the steel wall is presented, but it is only for validation purpose, and in practice it has limited use.

The electrical circuit analog of the overall heat transfer from the gas to the outside is shown in Figure 3. The energy equation for the thin material (steel plate) is:

$$\rho \delta c \frac{\partial T_w}{\partial t} = (h_{c1} + h_{r1})(T_g - T_w) - (h_{c2} + h_{r2})(T_g - T_o) \quad (11)$$

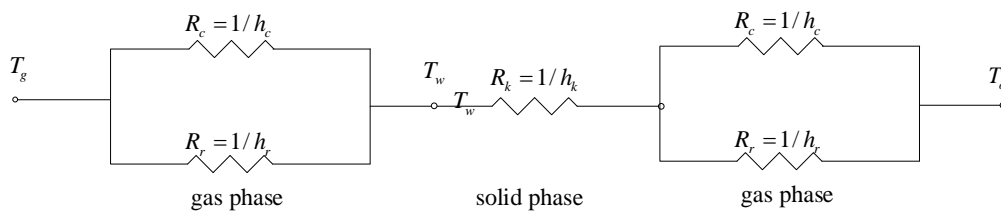


Figure 3 The electrical circuit analog of global heat transfer from gas to the wall.

For simplicity, the process can be assumed to be quasi-steady. Therefore, the heat flux into the steel is:

$$\dot{q}'' = h(T_g - T_o) \quad (12)$$

The heat transfer coefficient is therefore:

$$h = \frac{1}{1/(h_{c1} + h_{r1}) + 1/h_k + 1/(h_{c2} + h_{r2})} \quad (13)$$

where

$$h_{r1} = \sigma(T_g^2 + T_w^2)(T_g + T_w)/(1/\varepsilon_g + 1/\varepsilon_w - 1), \quad h_{r2} = \varepsilon_w \sigma(T_w^2 + T_o^2)(T_w + T_o), \quad h_k = \delta_s/k_s$$

The wall temperature can be estimated by:

$$T_w = T_g - \frac{h(T_g - T_o)}{h_c + h_r} \quad (14)$$

2.2.2 Parameter K_{ef}

The parameter, K_{ef} , is [1]:

$$K_{ef} = \frac{\dot{m}_g c_p}{A_w} = \frac{155AH_{ef}^{1/2}}{(1 + C_u)PH} \quad (15)$$

where

$$C_u = \begin{cases} 1 - 3.3u^* & u^* < 0.3 \\ 0 & u^* \geq 0.3 \end{cases} \quad \text{and} \quad u^* = \frac{u_o}{\sqrt{gH}}$$

2.2.3 Mass flow rate

If the HRR is not known, the fire is assumed to be fuel-rich (or ventilation-controlled). Thus, the mass flow rate is the amount of fresh air entering the tunnel. The total amount of fresh air that enters the tunnel by forced or natural ventilation, \dot{m}_g , could be estimated by the following correlation:

$$\dot{m}_g = \max(A\sqrt{H}, \rho_o u_o A) \quad (16)$$

If the HRR is known, a limit should also be used to estimate the mass flow rate of the flame volume. This mass flow rate could be estimated as follows:

$$\dot{m}_g = \frac{\dot{Q}}{c_p \Delta T_{ad}} \quad (17)$$

Therefore, the mass flow rate is:

$$\dot{m}_g = \min\left[\frac{\dot{Q}}{c_p \Delta T_{ad}}, \max(A\sqrt{H}, \rho_o u_o A)\right] \quad (18)$$

Note that the first term functions as a limit to the mass flow rate, and it should be used only when the gas temperature is high. It may be ignored in some cases and then the results obtained tend to be conservative.

2.2.4 Time correction

Note that the above equation is valid when a continuous flame impinges on the ceiling of the tunnel and the gas temperature is very high. However, fires generally have a longer growth period. In order to calculate the full expression of the gas temperature as a function of time, it is often necessary to compensate for the time in the growth period.

Before the continuous flame impinges on the ceiling, it may be assumed that the heat loss to the boundary, along with the limit for adiabatic flame temperature, do not significantly influence the maximum ceiling gas temperature, and thus the previous models apply (see Eqs. (1) and (2)). The point of distinction is estimated to be above the excess gas temperature of 900°C by comparison between test data and calculated values. Before this value is obtained, calculated gas temperature values do not deviate significantly from the previous MT model. This also fits well with the representative flame temperature value chosen for continuous flames in open fires. The scientific explanation for this is that, before this gas temperature is obtained, the influence of surrounding structures on changes in gas temperature is negligible, i.e. the time delay is relatively small. When the continuous flames impinge on the ceiling, the new MT model begins to apply.

If a design fire is known, according to the previous MT model, the time corresponding to a temperature of 900 °C, t_{01} , can be obtained, as the corresponding HRR can be estimated by the following equation:

$$\dot{Q}(t) = \max(H_{ef}^{5/2} (\frac{\Delta T}{17.5})^{3/2}, u_o b_{fo}^{1/3} H_{ef}^{5/3} \Delta T) \quad (19)$$

where ΔT_c is the excess gas temperature at the point of distinction, and time, t_{01} , is the point in time at which 800°C is obtained.

According to the new MT model, time, t_{02} , indicates how long it takes for the gas temperature (surface temperature) to reach 800°C if the structure is surrounded by large flames from the beginning. The corrected time used in the new MT model, i.e. Eq. (8), is therefore $(t+t_{02}-t_{01})$. The heat transfer coefficient is then obtained by:

$$h_k = \sqrt{\frac{k\rho c}{\pi t_c}} = \sqrt{\frac{k\rho c}{\pi(t+t_{02}-t_{01})}} \quad (20)$$

To estimate the time, t_{02} , a modified flame temperature is defined as follows:

$$\Delta T'_{ad} = \Delta T_{ad} - \varphi \varepsilon \sigma A (T^4 - T_o^4) / \dot{m}_g c_p \quad (21)$$

For a tunnel structure that is covered by a single material, the time, t_{02} , can be estimated using Eqs. (8), (20), and (36):

$$t_{02} = \frac{k\rho c}{\pi K_{ef}^2} \left(\frac{\Delta T}{\Delta T'_{ad} - \Delta T} \right)^2 \quad (22)$$

For a tunnel structure that is covered by N different materials, the time, t_{02} , can be simply estimated using:

$$t_{02} = \left[\sum_i^N (X_i \sqrt{\frac{(k\rho c)_i}{\pi}}) \right]^2 \frac{1}{K_{ef}^2} \left(\frac{\Delta T}{\Delta T'_{ad} - \Delta T} \right)^2 \quad (23)$$

If there are objects within the tunnel, the time can be estimated using:

$$t_{o2} = \left[\sum_i^N (X_i \sqrt{\frac{(k\rho c)_i}{\pi}}) + \frac{A_{object}}{A_w} \sqrt{\frac{(k\rho c)_i}{\pi}} \right]^2 \frac{1}{K_{ef}^2} \left(\frac{\Delta T}{\Delta T'_{ad} - \Delta T} \right)^2 \quad (24)$$

Here ΔT was set to 900°C in order to estimate the point of distinction. Based on a series of calculations that were conducted in order to estimate the time, t_{o2} , it was found that a value of 1500°C can be used for the modified flame temperature, $\Delta T'_{ad}$. However, a constant modified flame temperature is not recommended when performing general calculations of gas temperatures, as in reality the value generally decreases with time.

3 Model scale tunnel fire tests

The main purpose of the tests is to investigate the tunnel structure on gas temperatures inside the tunnel. The parameters tested include tunnel materials, cross sections, ventilation conditions and fire sources. Another purpose is to calibrate and validate the new MT models using the test data.

3.1 Tunnel

The tunnel was 10 m long, see Figure 1. In most of the tests, the tunnel cross section was 0.6 m (H) \times 0.6 m (W) but in some tests a wide tunnel with dimensions of 0.6 m (H) \times 1 m (W) was used. The values are all for internal dimensions. An axial fan was installed on the left side to produce a longitudinal flow along the tunnel.



Figure 4 A schematic diagram of the tunnel sections

The tunnel consisted of four 2.5 m long sections. The two sections nearby the fire site (gray in Figure 1) were made of either: light weight concrete (LWC), Mineral wool, Gypsum boards, Promatect H or steel sheet. The total interior surface area is either 10 m² or 15 m². The sections close to the two ends were constructed with Promatect H during the tests. The properties for the wall materials are shown in Table 1. The thickness varies following the scaling method proposed by Li and Hertzberg [5].

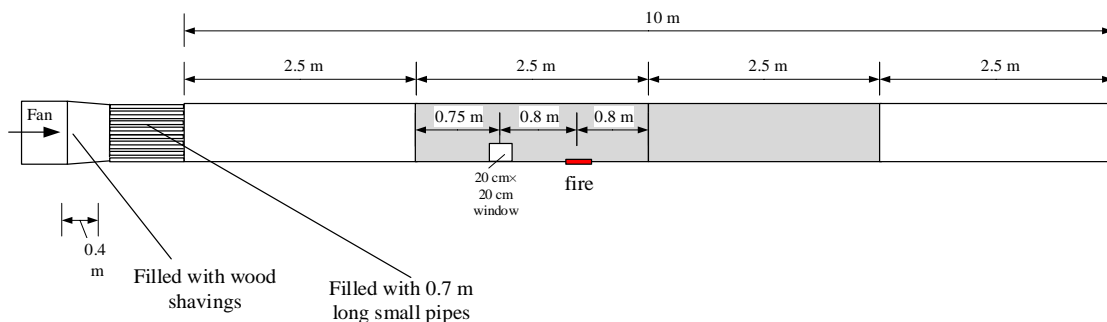


Figure 5 A schematic diagram of the tunnel sections

Table 1 Tunnel wall materials.

Tunnel material	Thickness of the material	Thermal conductivity	Density	Heat capacity	Thermal inertia
	mm	W/mK	kg/m ³	J/kgK	J ² /(m ⁴ K ² s)
Lightweight Concrete	100	0.16	647	835	8.64E+04
Promatect H	35	0.19	870	1130	1.87E+05
Mineral wool	60	0.038	170	750	4.85E+03
Gypsum boards	60	0.17	800	1000	1.36E+05
Steel	2	43	7800	473	1.59E+08

3.2 Fire source

In most of the tests, a gas burner with dimensions of 20 cm × 20 cm was used on the floor as the fire source. In some tests, liquid pools were used with dimensions of 20 cm × 25 cm (5 cm depth) and 30 cm × 35 cm (6 cm depth). The small pool was filled with 1.5 l of heptane. The large pools were filled with 4.2 l of heptane.

3.3 Ventilation

An axial fan was installed on the left side to produce a longitudinal flow along the tunnel. The longitudinal velocity in the tunnel is either around 1 m/s or around 0.6 m/s. The corresponding full scale velocities are 3.2 m/s and 1.9 m/s. These correspond to one scenario close to critical condition and another scenario with a certain length of backlayering, according to the previous study [6].

3.4 Measurement

The measurements inside the tunnel are shown in Figure 6. Thermocouples, bi-directional pressure tubes, gas analysis and plate thermometers were used to measure the gas temperature and pressure, gas concentrations and radiation heat flux, respectively. All ceiling thermocouples were placed 5 cm below the ceiling, except at Pile C (4.3 m downstream). At Pile C, 3 gas analysis probes were placed at the centreline of the tunnel, and the bi-directional tubes and thermocouples were placed horizontally 5 cm from the gas analysis. One plate thermometer was placed beneath the ceiling at Pile C. In some tests another plate thermometer was placed right beside the fire source to measure the flame heat flux.

Note that the thermocouple T21 was placed 20 cm horizontally from the thermocouple T5.

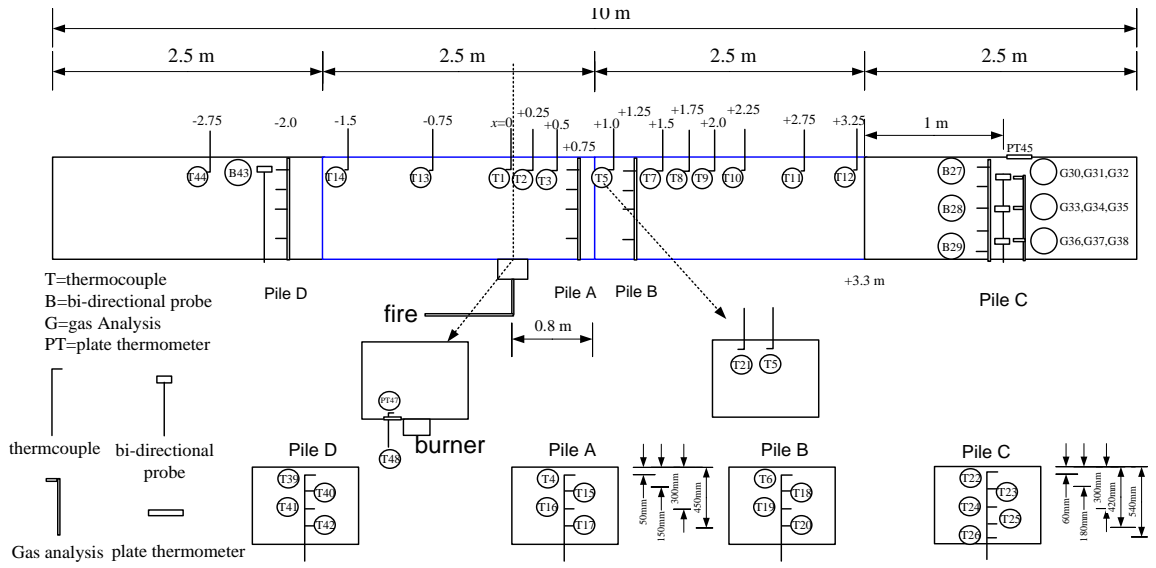


Figure 6 Test measurements and instrumentations.

3.5 Test procedure

Six series of tests were carried out using six different lining materials inside the tunnel. Either the material of the fire section or the width of the tunnel varies between the test series. In each series of tests, fire source type and fire size were applied. Additionally, a pre-test was conducted before these six series of tests to check all the measurements. In total 39 fire tests were carried out during these six different test series.

Test series	Test no.	Tunnel lining material	Fuel	HRR	velocity
				kW	m/s
Pre-test	001	Gypsum boards	Gas	30	0.6
Test series 1	101	Gypsum boards	Gas	450	1.0
	102	Gypsum boards	Small Pool	93	1.0
	103	Gypsum boards	Large Pool	380	1.0
	104	Gypsum boards	Gas	450	0.6
Test series 2	201	Steel sheet	Small Pool	93	1.0
	202	Steel sheet	Gas	150	1.0
	202B*	Steel sheet	Gas	150	1.0
	203	Steel sheet	Gas	300	1.0
	204	Steel sheet	Gas	450	1.0
	205	Steel sheet	Gas	450	0.6
Test series 3	206	Steel sheet	Large Pool	250	1.0
	301	Mineral wool	Small Pool		1.0
	302	Mineral wool	Gas	450	1.0
	303	Mineral wool	Large Pool		1.0
Test series 4	304	Mineral wool	Gas	450	0.6
	401	Promatect H	Small Pool		1.0
	402	Promatect H	Small Pool		0.6
	403	Promatect H	Large Pool	400	1.0
	404	Promatect H	Gas	450	1.0
Test series 5	405	Promatect H	Gas	450	0.6
	501	LWC	Small Pool		1.0
	502	LWC	Small Pool		0.6
	503	LWC	Large Pool	400	1.0
	504	LWC	Large Pool	400	0.6
	505	LWC	Gas	450	1.0
	506	LWC	Gas	450	0.6
	507	LWC	Gas	300	1.0
508	LWC	Gas	300	0.6	
Test series 6 – Wide tunnel	601	LWC, wide	Small Pool	93	1.0
	602	LWC, wide	Small Pool	93	0.6
	603	LWC, wide	Large Pool	400	1.0
	604	LWC, wide	Large Pool	400	0.6
	605	LWC, wide	Gas	300	1.0
	606	LWC, wide	Gas	300	0.6
	607	LWC, wide	Gas	450	0.6
	608	LWC, wide	Gas	450	1.0
	609	LWC, wide	Gas	520	1.0
	610	LWC, wide	Gas	600	0.6
	611	LWC, wide	Gas	600	1.0

* A repeat of Test 202.

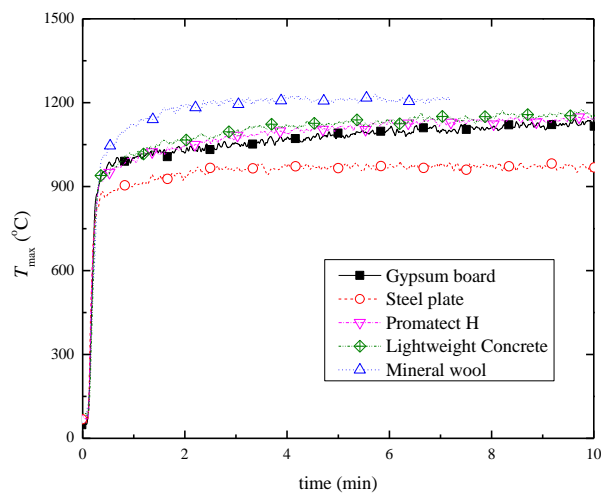
4 Results and discussions

In the following, test results on maximum ceiling gas temperatures (among T1-T12) are shown and then compared with model predictions. Besides, data from some other model scale and some full scale tests are used for comparison with the model predictions.

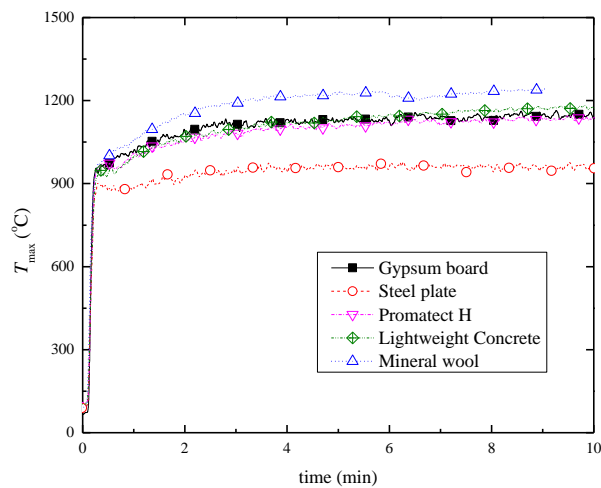
4.1 Test results

4.1.1 Influence of tunnel structure materials

Figure 7 shows the results on maximum ceiling gas temperature with various tunnel structure materials. By comparing the results with the thermal inertias of the materials for both 1 m/s and 0.6 m/s, it can be found that the maximum gas temperatures are higher for a more fire resistant material (with a lower thermal inertia). This is due to the fact that the heat loss to the inner side of the material becomes smaller due to the lower thermal inertia. The values for mineral wool are around 100 °C higher than those for Gypsum board, Promatect and Lightweight Concrete.



(a) 1 m/s

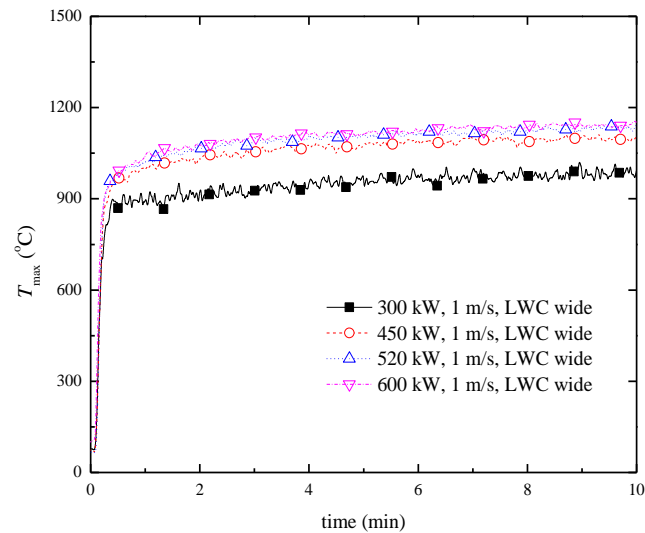


(b) 0.6 m/s

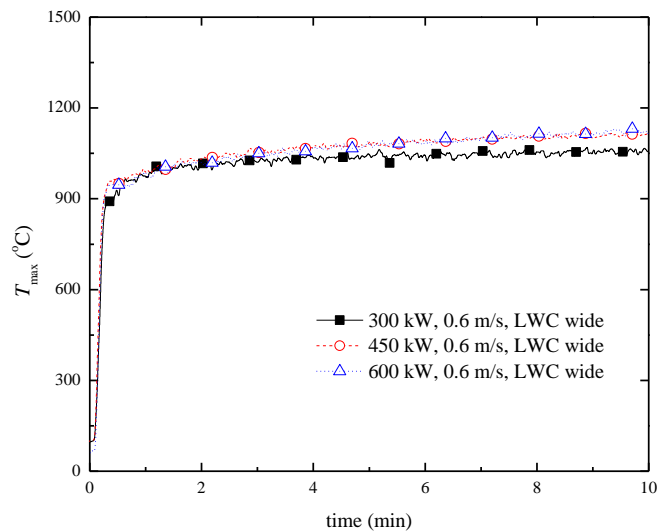
Figure 7 Influence of tunnel structure materials on maximum gas temperature (MT).

4.1.2 Influence of fire size

Figure 8 shows the influence of fire size on the maximum ceiling gas temperatures in the wide tunnel with lightweight concrete (LWC). Clearly, it shows that the maximum gas temperature increases with the increasing heat release rate. At a velocity of 1 m/s, the maximum ceiling gas temperature for 300 kW (95 MW in full scale) is much lower than the others, and the differences become smaller for larger fires. In contrast, at a velocity of 0.6 m/s, the same trend can be found but the differences in maximum ceiling gas temperature for different fire sizes are much smaller.



(a) 1 m/s



(b) 0.6 m/s

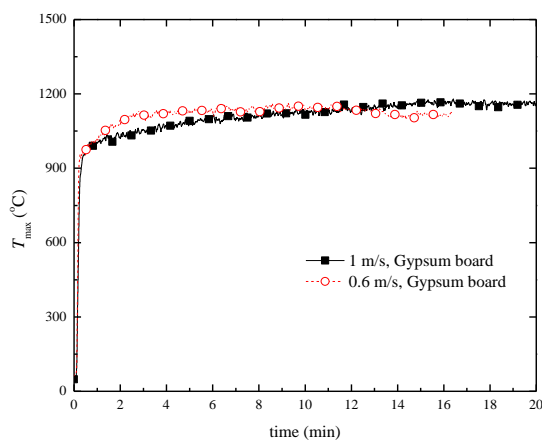
Figure 8 Influence of fire size on MT.

4.1.3 Influence of ventilation

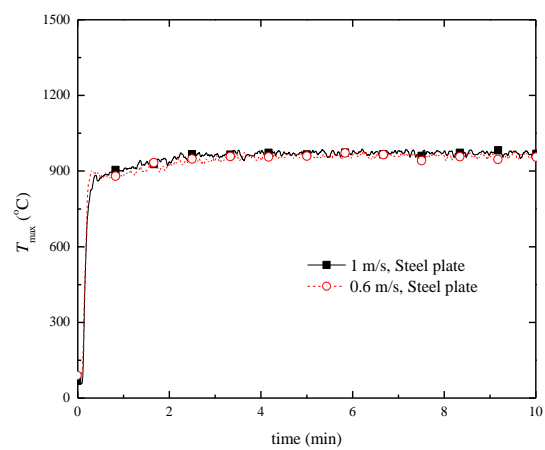
Figure 9 shows the results on maximum ceiling gas temperature with different ventilation velocities for various tunnel structure materials and heat release rate of 450 kW.

It can be seen from Figure 9 that, in general, the influence of ventilation on the maximum gas temperatures in the tunnels appears to be insignificant. For steel and Promatect, there seems to be a trend that the gas temperature for 1 m/s is slightly higher than that for 0.6 m/s. For all the materials, the maximum temperature for 0.6 m/s is lower at the early stage of the fire.

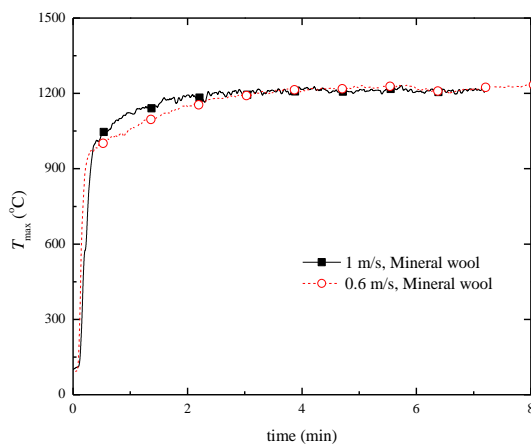
In tests with gypsum board, the temperatures for 0.6 m/s are higher during the first 8 min. The reason could be that the gypsum boards became more thermal resistant in the tests with 0.6 m/s, given that this test was carried out at the end of the test series while the test with 1 m/s was carried out at the beginning of the test series where the gypsum boards contain significant amounts of moisture.



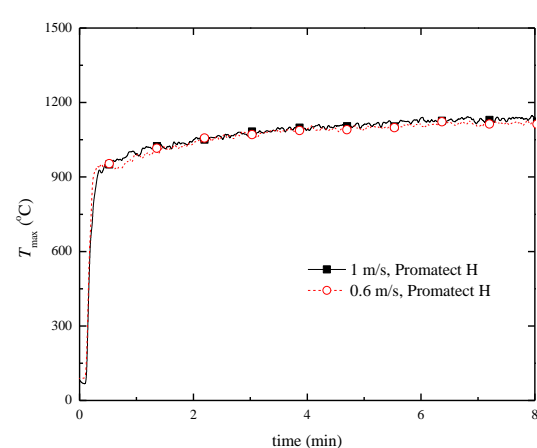
(a) Gypsum board



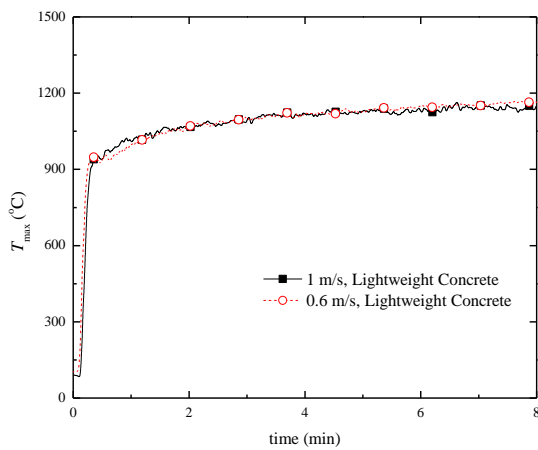
(b) steel



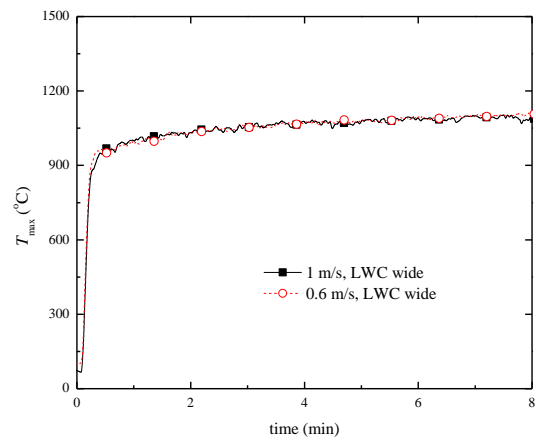
(c) Mineral wool



(d) Promatect H



(e) Lightweight concrete LWC



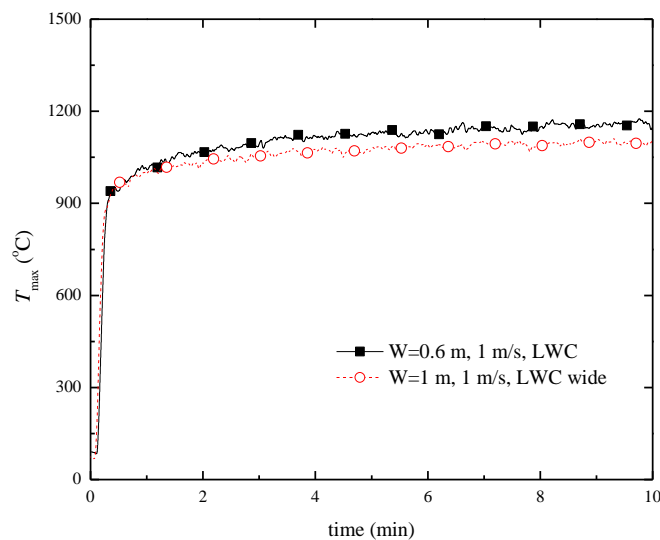
(f) LWC, wide tunnel

Figure 9 Influence of ventilation on MT for various materials (450 kW).

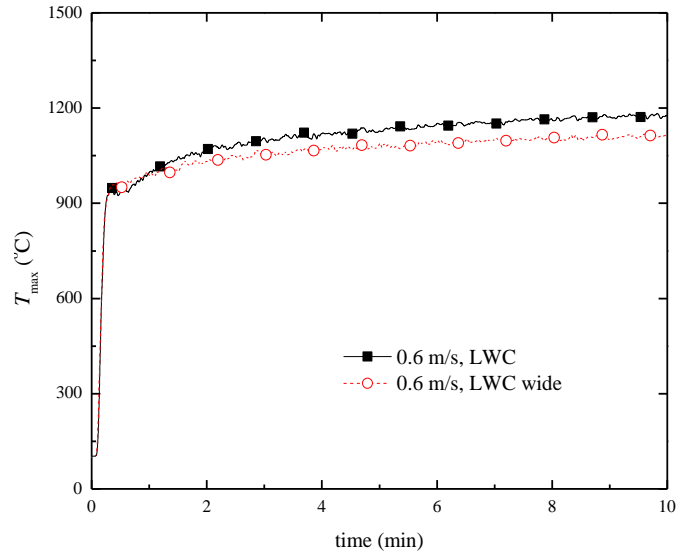
4.1.4 Influence of tunnel width

Figure 10 shows the results on maximum ceiling gas temperature in tunnels with different widths for velocities of 1 m/s and 0.6 m/s and a heat release rate of 450 kW.

Clearly, it shows in Figure 10 that for both 1 m/s and 0.6 m/s, the maximum gas temperature decreases with the increasing tunnel width. This is mainly due to the larger heat loss to the surrounding for a wider tunnel.



(a) 1m/s



(b) 0.6m/s

Figure 10 Influence of tunnel width on MT under various ventilation velocities (450 kW).

4.2 Comparisons to theoretical models

In the predictions, an effective emissivity obtained from model scale tests is used. This emissivity could be estimated by the following correlation:

$$\varepsilon = \frac{\dot{q}_{inc}''}{\sigma T^4} \quad (25)$$

In most of the model scale tests, it is found that this emissivity is around 0.6. Note that in full scale tests, this emissivity is around 1 [4].

4.2.1 Calculation of heat transfer coefficient

Here we examine the reasonability of using Eq. (6) as the heat transfer coefficient. Figure 11 shows the comparisons of the maximum ceiling gas temperatures in the lightweight concrete tunnel with the model predictions with two different calculation methods, i.e. a complete calculation of lumped heat transfer coefficient, h , with Eq. (8), and the simplified calculation of the heat transfer coefficient, h_k , with Eq. (6).

It is shown in Figure 11 that the difference in the temperatures from the complete and simplified calculations is negligible. Therefore, the simplified calculation, i.e. Eq. (6) can be used in these cases with thermally thick materials. Only in the tests with steel, the special method, i.e. Eq. (13), is needed.

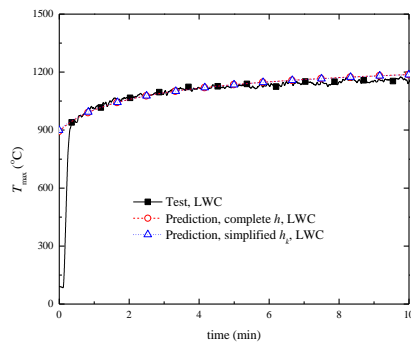
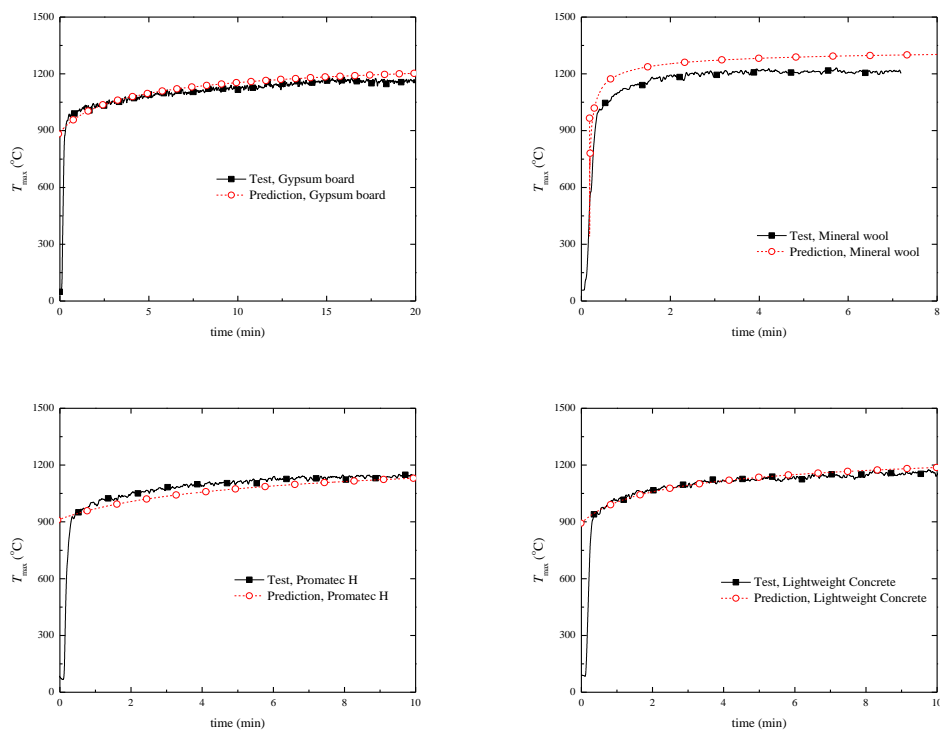


Figure 11 Difference between the two calculation methods for heat transfer coefficient.

4.2.2 Tunnel structure and ventilation

Figure 12 shows the comparisons of the measured and predicted maximum ceiling gas temperatures in tunnels of various materials and a heat release rate of 450 kW under velocities of 1 m/s and 0.6 m/s. The results are mostly correlate very well for both 1 m/s and 0.6 m/s. Overall, the variations of maximum temperature with tunnel structure and ventilation are well predicted.

One exception is the mineral wool tunnel where the maximum temperatures are overestimated to some extent. This may be attributed to the fact that the mineral wool generally shrinks after exposed to high temperature and it even melts around 1200 °C (see Figure 13), causing variations in the physical and thermal properties of the material.



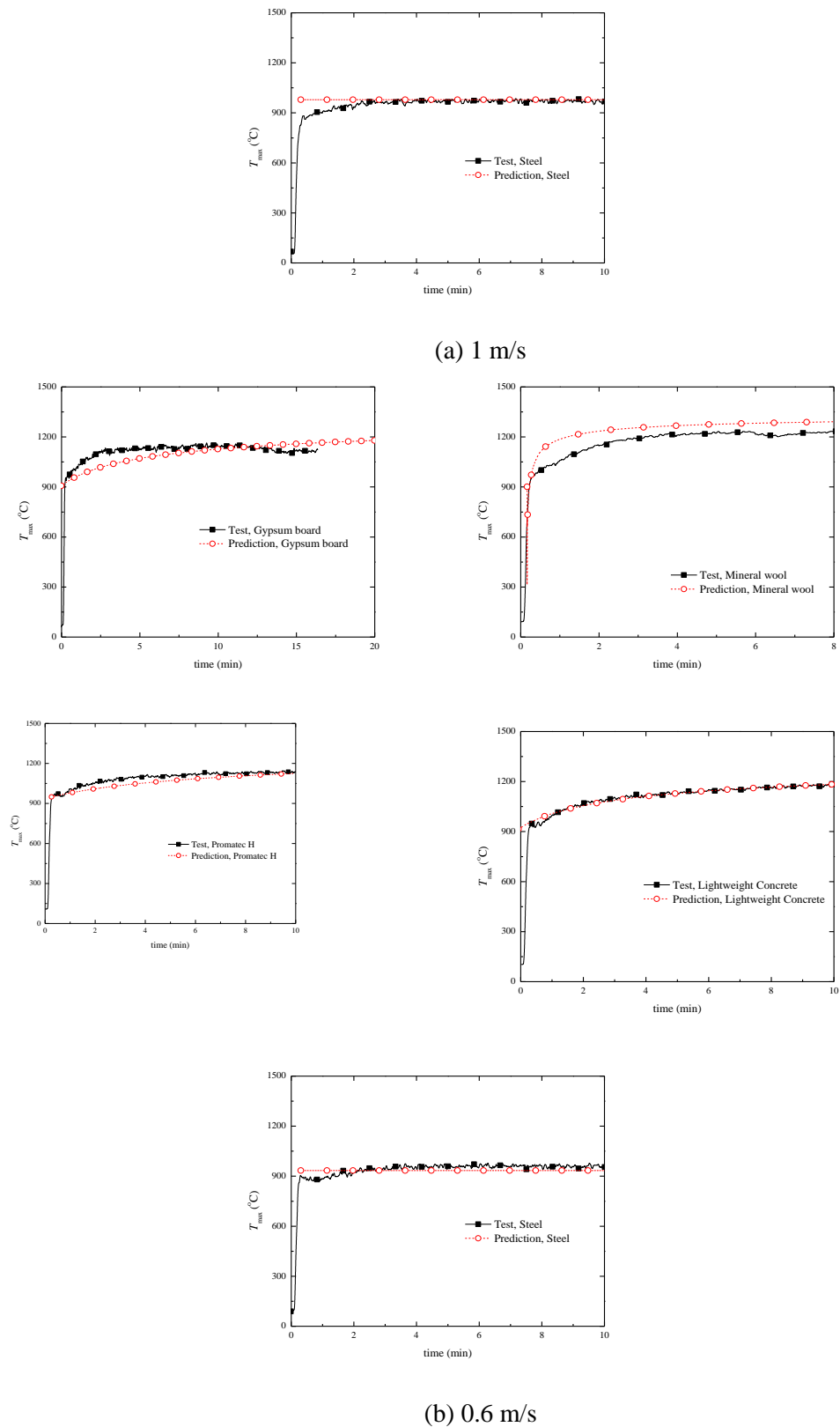


Figure 12 Influence of tunnel structure materials on MT ($Q=450$ kW).

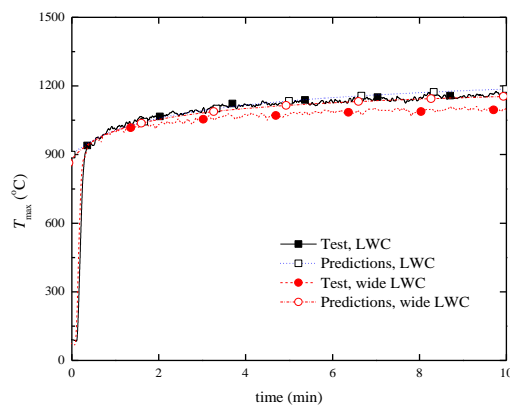


Figure 13 A photo of the mineral wool after the test.

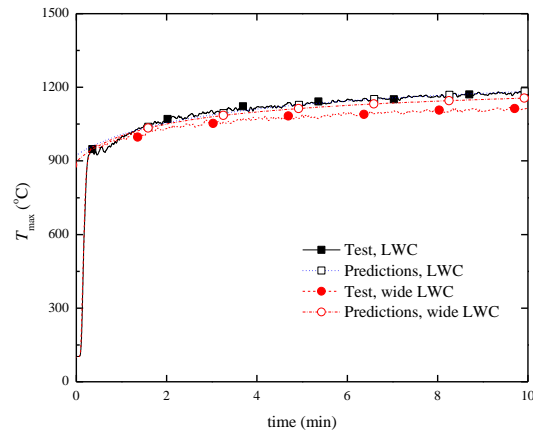
4.2.3 Tunnel width

Figure 14 shows the comparisons of the measured and predicted maximum ceiling gas temperatures in tunnels of various widths and a heat release rate of 450 kW under velocities of 1 m/s and 0.6 m/s.

The variations of maximum temperature with tunnel width are well predicted. Both results show that the maximum temperature is slightly higher for the narrower tunnel. Further, the predictions are slightly higher than measured values, indicating the predictions tend to be conservative.



(a) 1m/s



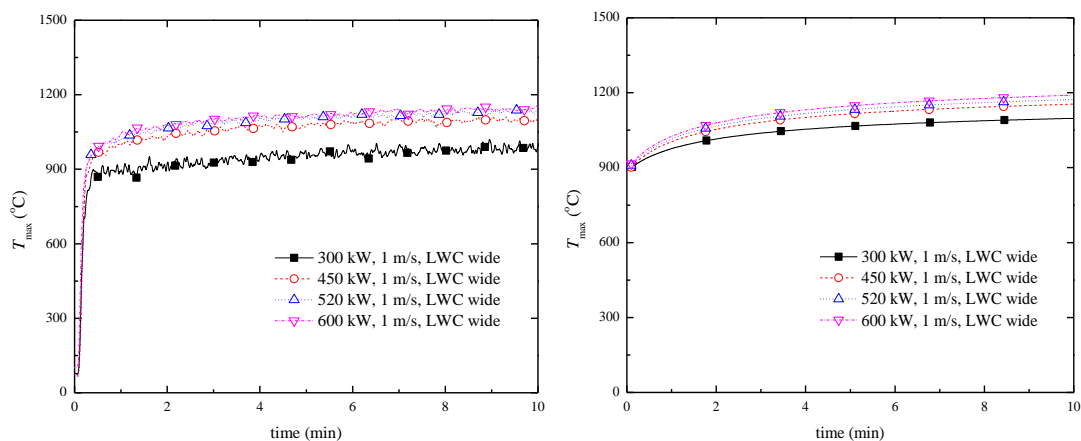
(b) 0.6m/s

Figure 14 Influence of tunnel width on MT ($Q=450$ kW).

4.2.4 Fire size HRR

Figure 15 shows the comparisons of the measured and predicted maximum ceiling gas temperatures in tunnels of various fire sizes for velocities of 1 m/s and 0.6 m/s.

It is shown from both test data and predictions in Figure 15 that the gas temperature increases with the increasing heat release rate, and the differences are very small for fires over 450 kW. The variation of maximum temperature with fire size has been well predicted. It can also be noticed that the predicted gas temperature is slightly higher than test data for 300 kW at 1 m/s. This indicates that the calculated results tend to be conservative.



(a) 1 m/s

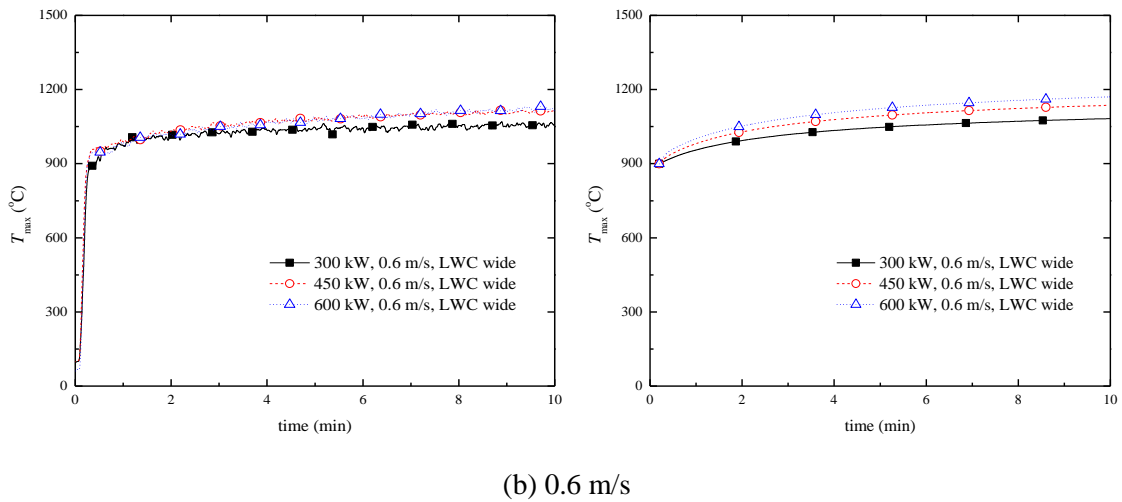
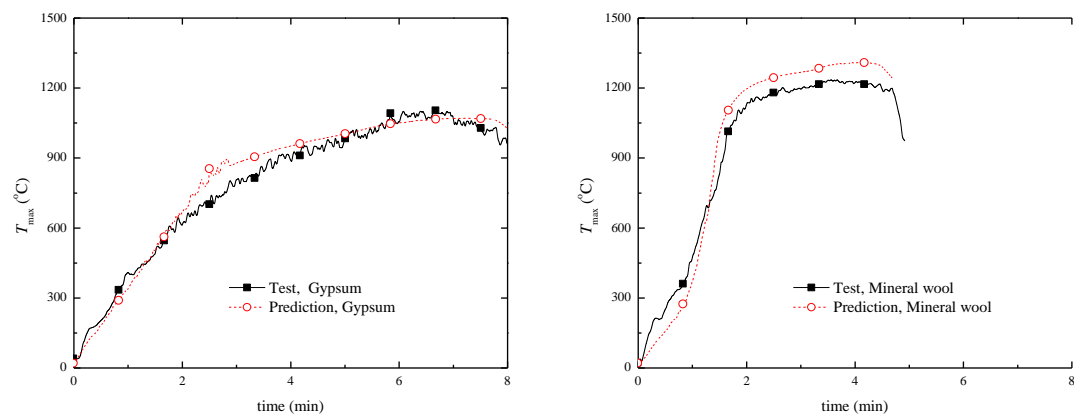


Figure 15 Influence of fire size HRR on MT.

4.2.5 Pool fires with varying HRRs

Figure 16 shows the comparisons of the measured and predicted maximum ceiling gas temperatures in tunnels with pool fires for various materials. The tests all correspond to the “large pool”. Note that for a pool fire, the heat release rate is not a fixed value, and instead it can vary with time significantly in the early stage. The time-varying heat release rates are used as inputs for the predictions.

It shows in Figure 16 that there is a good agreement between the measured and predicted maximum ceiling gas temperature during the whole burning periods. In some figures, overestimations can be found. This may be attributed to possible overestimations of heat release rates. It may also indicate that the predictions tend to be conservative.



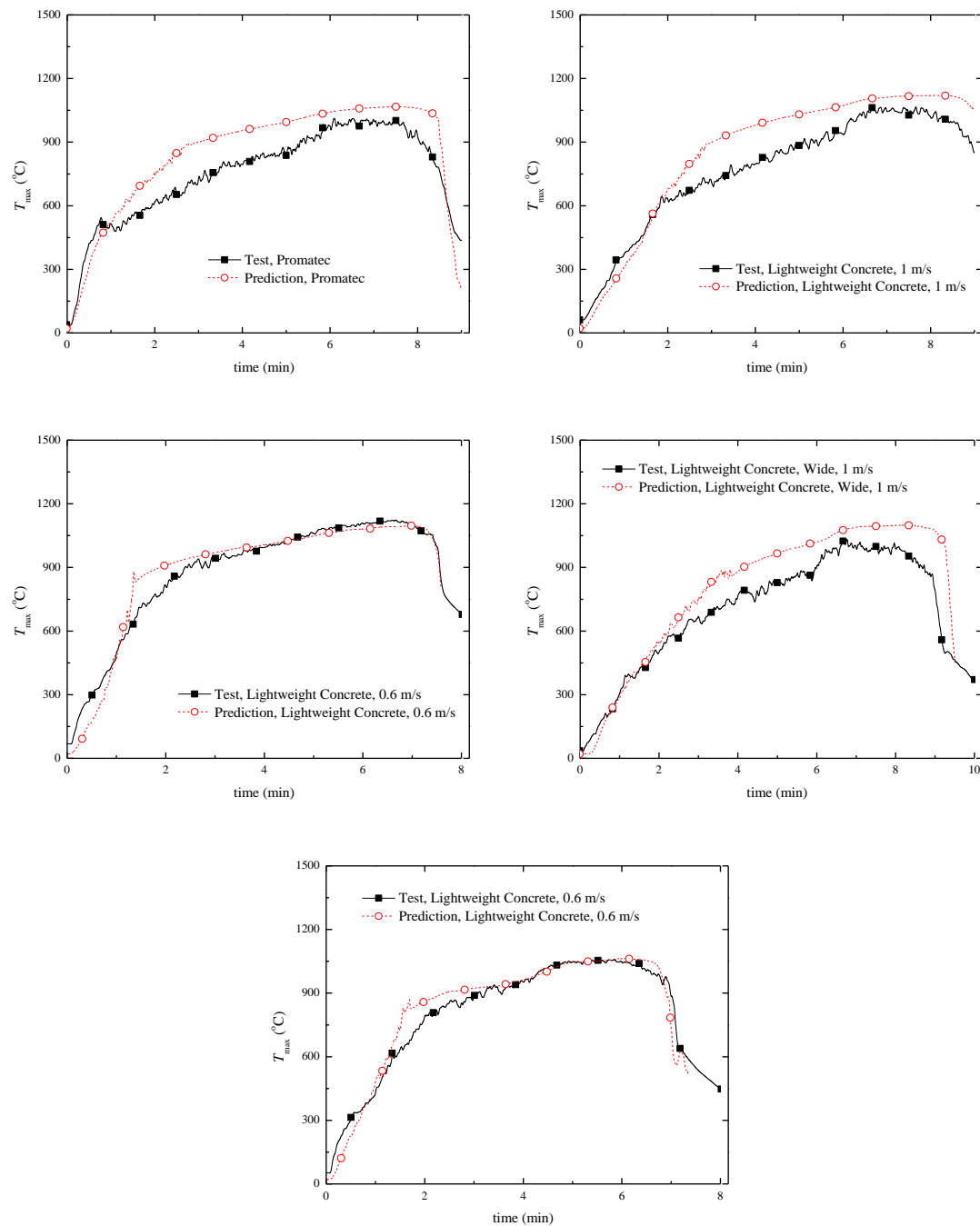


Figure 16 Comparison of measured and predicted MT for pool fires (Large pool).

4.3 Comparison to other model scale tests

One test from the model-scale tests (Test 905) is used here for comparison, where the model tunnel was 12.5 m long (14.5 m if the fan section is included), 0.6 m high, and 0.6 m wide [7]. The model tunnels were constructed using 4 cm thick non-combustible Calcium silicate boards (Promatect L), with the exception of the lower part (50%) of one side of the tunnel, which was covered with a fire-resistant window panel, mounted on steel frames. The Promatect L has a conductivity of $0.083 \text{ W/m} \cdot \text{K}$, a density of 450 kg/m^3 , a heat capacity of $1130 \text{ J/kg} \cdot \text{K}$, and a

thermal inertia, $k\rho c$, of approximately $4.2 \times 10^4 \text{ W}^2\text{sm}^{-4}\text{K}^{-2}$. The material was chosen according to the scaling theory proposed by Li and Hertzberg [8] in order to simulate the concrete and rock that are used in tunnels (or a mixture of dense and medium-dense concrete).

Figure 17 shows the comparison of the measured and predicted maximum ceiling gas temperature for test 905 with 632 kW. In test 905, the fire size was kept constant as 632 kW for 8.5 min while the velocity varies from 2 m/s to 1 m/s at 3 min and further to 0.5 m/s at 6 min. The HRR curves and average flow velocities were used to produce time-temperature curves

It clearly shows in Figure 17 that there is a good agreement between them. Measured and predicted data both shows that there is a slight drop in the temperature at 3 min, and a much clearer drop at 6 min.

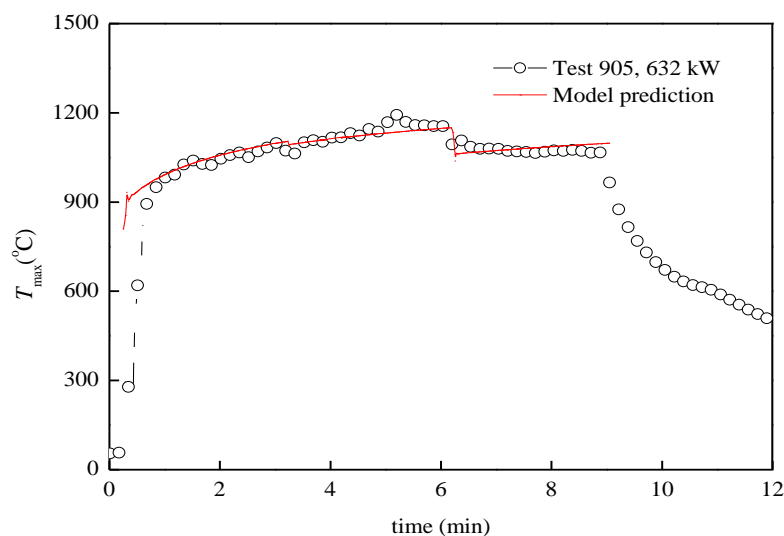


Figure 17 A comparison of the calculated transient maximum temperature beneath the ceiling and the data obtained during Runehamar Test 2. 2 – 1 – 0.5 m/s.

4.4 Comparison to full scale tests

The full scale Runehamar tunnel Fire Tests 1-4 [4, 9] are used here for comparison of the maximum ceiling gas temperatures. The fire tests were carried out using HGV (Heavy Goods Vehicle) mock-ups in the Runehamar tunnel, Norway, in 2003. In the vicinity of the fire sources, the tunnel walls and ceiling were covered with Promatect T boards with a thermal inertia of approximately $1.9 \times 10^5 \text{ W}^2\text{sm}^{-4}\text{K}^{-2}$; the floor is made of asphalt.

The HRR curves and average flow velocities were used to produce time-temperature curves, which are shown in Figure 18, Figure 19, Figure 20 and Figure 21. Note that in full scale tests, this emissivity is around 1 [4].

It should be noted that, in Test 1, all of the measurements worked well during the entire test, but in Tests 2 and 3, the thermocouple located 10 m downstream of the fire worked well during the early stages of the test, but failed after around 10 min. Therefore, the maximum gas temperatures are not known after that point in time.

The calculated gas temperature curves correlate well with the measured temperature curves and the maximum gas temperatures are well predicted. It can also be observed that the measured temperature rose much more rapidly during Test 3, which was likely the result of a measurement error at the early stage of the test. It should be noted that the fire grew extremely rapidly in this test with polyurethane foams, as compared to the others. Furthermore, the measuring of the HRR was performed 463 m downstream of the fire site. Therefore, during the rapidly growing period, the transportation of the combustion products to the measurement station could cause a relatively larger error as compared to the other tests. In addition, the fire radius is considered to be a constant in the calculation, i.e. the largest fire radius is used, but varies with fire size. A smaller fire radius results in higher gas temperatures, according to the model. This indicates that the temperature may be underestimated if the equivalent radius of the whole fire source is used to predict the temperature at the early stage of a large fire.

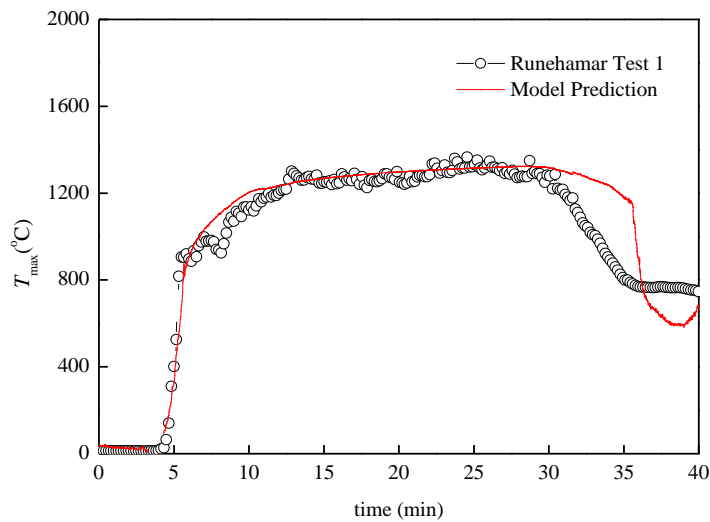


Figure 18 A comparison of the calculated transient maximum temperature beneath the ceiling and the data obtained during Runehamar Test 1.

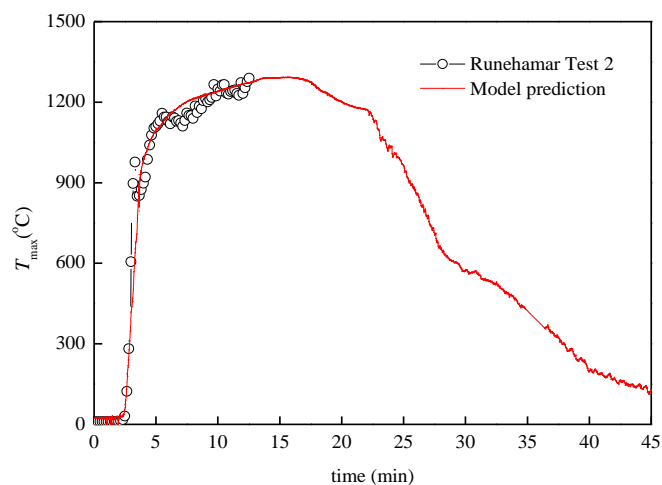


Figure 19 A comparison of the calculated transient maximum temperature beneath the ceiling and the data obtained during Runehamar Test 2.

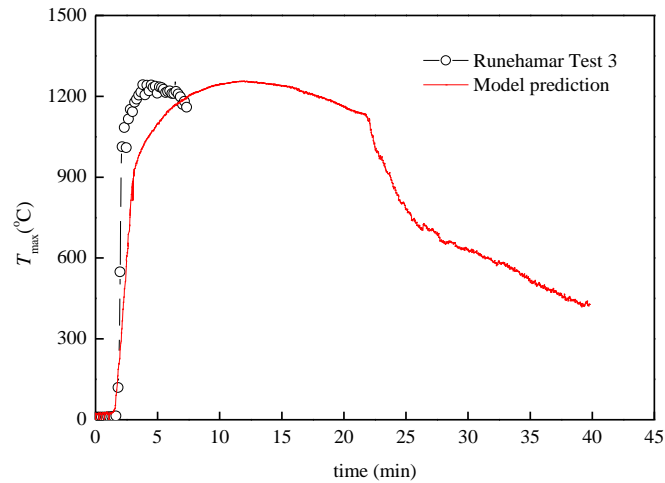


Figure 20 A comparison of the calculated transient maximum temperature beneath the ceiling and the data obtained during Runehamar Test 3.

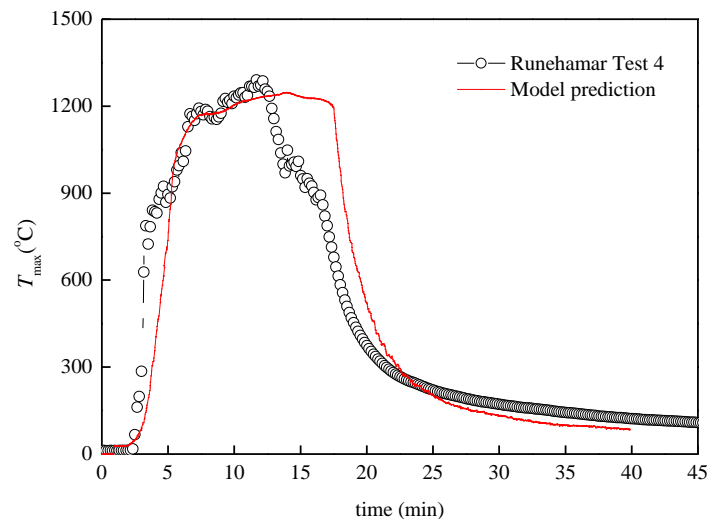


Figure 21 A comparison of the calculated transient maximum temperature beneath the ceiling and the data obtained during Runehamar Test 4.

4.5 Summary of the new MT model

The comparisons show good agreement between the measured and predicted results of maximum ceiling gas temperature in tunnel fires, whether it is a fire with a fixed heat release rate or a time-varying heat release rate.

The calculations show that the heat transfer coefficient can be estimated using Eq. (6) for thermally thick materials which are the cases for realistic tunnel fires. The correction factor, ϕ , of 1 is reasonable for the prediction. The emissivity in the full scale is around 1, while it is smaller in model scales (mostly around 0.6 for a scale ratio between 1:20 and 1:10). Calculation methods for the parameter, K_{ef} , and the time correction are proven to be reasonable.

5 Conclusions

Several test series with varying lining materials in the tunnel structure were carried out to further study the theoretical model of maximum gas temperature for structural protection recently presented by the authors. New correlation for calculation of mass flow rate is introduced.

Analysis of the test results showed that the maximum gas temperatures become higher for a more fire-resistant material (with a lower thermal inertia). The maximum gas temperature increases with the increasing heat release rate, but this increase becomes smaller as the heat release rate continues to rise. This increase depends on the ventilation velocity, and it is smaller for a lower velocity. The influence of different ventilation conditions tested is not significant. It appears to be a trend that higher ventilation may result in slightly higher temperatures for large fires. The maximum gas temperature decreases with the increasing tunnel width due to greater heat loss to environment. Overall, the maximum ceiling gas temperatures increases with the increasing heat release rate and decreases with the increasing tunnel width and thermal inertia of the tunnel linings. Higher ventilation may also result in slightly higher temperatures for large fires.

Comparisons of model scale tests and theoretical models showed that the theoretical models predict the maximum ceiling gas temperature very well, whether it is a fire with a fixed heat release rate or a time-varying heat release rate. The effects of tunnel structure, tunnel ventilation, tunnel width and fire size have been well considered by the model. Comparisons of other model and full scale tests with theoretical models further verified this.

Reference

1. Li Y.Z., Ingason H., *New models for calculation of maximum gas temperatures in large tunnel fires*. 2016, SP Report 2016:95, SP Technical Research Institute of Sweden: Borås, Sweden.
2. Li Y.Z., Lei B., Ingason H., *The maximum temperature of buoyancy-driven smoke flow beneath the ceiling in tunnel fires*. *Fire Safety Journal*, 2011. **46**(4): p. 204-210. DOI: 10.1016/j.firesaf.2011.02.002.
3. Li Y.Z., Ingason H., *The maximum ceiling gas temperature in a large tunnel fire*. *Fire Safety Journal*, 2012. **48**: p. 38-48.
4. Ingason H., Li Y.Z., Lönnemark A., *Runehamar Tunnel Fire Tests*. *Fire Safety Journal*, 2015. **71**: p. 134–149.
5. Li Y.Z., Hertzberg T., *Scaling of internal wall temperatures in enclosure fires*. *Journal of Fire Sciences*, 2015. **33**(2): p. 113-141. DOI: 10.1177/0734904114563482.
6. Li Y.Z., Ingason H., *Effect of cross section on critical velocity in longitudinally ventilated tunnel fires*. *Fire Safety Journal*, 2017. **91**: p. 303–311.
7. Ingason H., Appel G., Gehandler J., Li Y.Z., Nyman H., Karlsson P., and Arvidson M., *Development of a test method for fire detection in road tunnels*. 2015, SP Technical Research Institute of Sweden, SP Report 2014:13: Borås.
8. Li Y.Z., Hertzberg T., *Scaling of internal wall temperatures in enclosure fires*. *Journal of Fire Science*, 2015. **33**(2): p. 113-141.
9. Ingason H., Lönnemark A., Li Y.Z., *Runehamar Tunnel Fire Tests*. 2011, SP Technical Research Institute: SP Report 2011:55.

Through our international collaboration programmes with academia, industry, and the public sector, we ensure the competitiveness of the Swedish business community on an international level and contribute to a sustainable society. Our 2,200 employees support and promote all manner of innovative processes, and our roughly 100 testbeds and demonstration facilities are instrumental in developing the future-proofing of products, technologies, and services. RISE Research Institutes of Sweden is fully owned by the Swedish state.

I internationell samverkan med akademi, näringsliv och offentlig sektor bidrar vi till ett konkurrenskraftigt näringsliv och ett hållbart samhälle. RISE 2 200 medarbetare driver och stöder alla typer av innovationsprocesser. Vi erbjuder ett 100-tal test- och demonstrationsmiljöer för framtidssäkra produkter, tekniker och tjänster. RISE Research Institutes of Sweden ägs av svenska staten.



RISE Research Institutes of Sweden
Box 857, 501 15 BORÅS
Telefon: 010-516 50 00
E-post: info@ri.se, Internet: www.sp.se / www.ri.se

Safety and Transport
RISE Rapport 2018:58
ISBN 978-91-88907-02-8
ISSN 0284-5172